

Shell forms for egg-shaped concrete sludge digesters: A comparative study on structural efficiency

A. Zingoni†

*Department of Civil Engineering, University of Cape Town,
Rondebosch 7701, Cape Town, South Africa*

(Received January 27, 2004, Accepted October 14, 2004)

Abstract. The structural feasibility of a variety of non-conventional sludge digesters, in the form of thin shells of revolution constructed in concrete, has formed the subject of investigation of a recent programme of research at the University of Cape Town. Such forms are usually known in the literature as “egg-shaped”, and the advantages of these over conventional digesters of the wide-cylindrical type are now well-recognised: superior mixing efficiency, less accumulation of deposits at the bottom, easier removal of bottom deposits and surface crust, reduced heat losses, and so forth. With the aim of exploring the structural feasibility of various non-conventional forms for concrete sludge digesters, and making available usable analytical data and practical guidelines for the design of such thin shell structures, a number of theoretical studies have recently been undertaken, and these have covered conical assemblies, spherical assemblies and parabolic ogival configurations. The purpose of the present paper is to bring together the different analytical approaches employed in each of these studies, summarise the main findings in each case, draw comparisons among the various studied configurations with regard to structural efficiency and functional suitability, and make appropriate conclusions and recommendations.

Key words: shell structures; containment shells; concrete digesters; shells of revolution; non-conventional sludge digesters; shell analysis; shell design.

1. Introduction

As is now well-recognised, non-conventional sludge digesters in the form of vertically-elongated shells of revolution of smoothly-varying meridional profiles with rounded ends (giving the so-called “egg-shape”), and variants of these with pointed ends (ogival shells) or straight-segmented meridional profiles (conical assemblies), offer several operational advantages in comparison with conventional sludge digesters in the form of squat cylindrical tanks with flat or domical tops and gently sloping conical bottoms. Most of these advantages stem from the superior sludge-mixing characteristics of the egg shape in comparison with the conventional shape (Fig. 1).

The vertically-elongated smooth profile of the egg shape is conducive to good circulation of the sludge, ensuring that the accumulation of sludge at the bottom of the digester is minimised. The little deposits that do collect at the bottom are easy to remove as they collect in a relatively small area, and the removal of these deposits may be carried out on a continuous basis. The removal of

† Professor, E-mail: azingon@eng.uct.ac.za

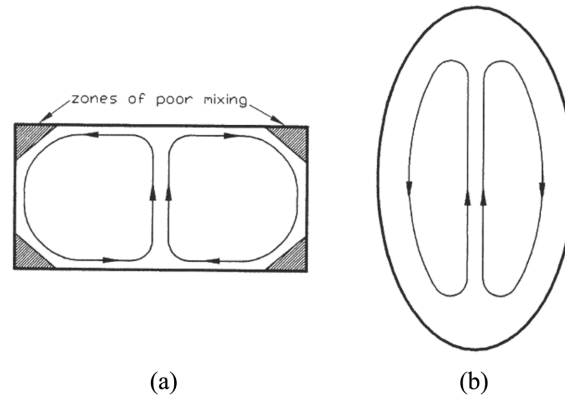


Fig. 1 Typical mixing patterns in sludge digesters: (a) conventional cylindrical digester, (b) egg-shaped digester

the crust that forms on the surface of the sludge is also facilitated by the tapered shape of the egg shape. Other advantages include lower heat losses (owing to the smaller surface-to-volume ratio of the egg shape relative to that of the cylindrical shape), higher methane-generating capacity (for use in heating the sludge to optimum digester operating temperatures), and a generally more elegant appearance (despite the higher profile of the egg shape). All this adds up to reduced maintenance costs over the long term, despite the higher initial construction costs of the egg shape, and these advantages have been exploited in countries such as Japan, Taiwan, Australia, Germany and the USA (Nojiri 1989, Aeberhard 1989, Sutter and Jager 1994, Jager 1997).

A recent programme of research at the University of Cape Town has focussed upon the structural feasibility of non-conventional sludge digesters in the form of thin shells of revolution constructed in concrete. Noting the scarcity of detailed and systematic information on the structural analysis of such structures, the efforts have centred around developing appropriate analytical methods for the problems in question, generating closed-form results for practical use, conducting parametric studies to allow general trends in structural behaviour to be established, and proposing recommendations for design. The studies have initially focussed on the effects of hydrostatic loading.

As part of this programme of research, a study was undertaken of a “true” egg shape in the form of a shell of revolution consisting of spherical top and bottom closures of radius a and half-angle of opening ϕ_0 (this angle being typically 45° to 70°), connected by an ogival middle portion of meridional radius of curvature A , as shown in Fig. 2(a). The spherical ends were assumed to meet the middle part tangentially, implying a discontinuity in meridional radius of curvature, but not in slope, at the junctions. Of interest in the study were the membrane stresses generated in the shell as a result of the contained hydrostatic internal pressure, and, in particular, the discontinuity stresses that occur at the junctions of the various regions. The theoretical approach, closed-form analytical results, conclusions and design recommendations have been reported in two related papers (Zingoni 2001a,b).

Another configuration that has been studied is the parabolic ogival shell (Fig. 2b), where the shell of revolution is formed by rotating a parabola that is symmetrical about the horizontal x axis, about the vertical y axis (which therefore is the axis of revolution of the shell). With its bulging middle and pointed ends, this shape seems well-suited for high-capacity sludge containment, and easy removal of both surface crust and bottom deposits. Moreover, the absence of loading and geometric

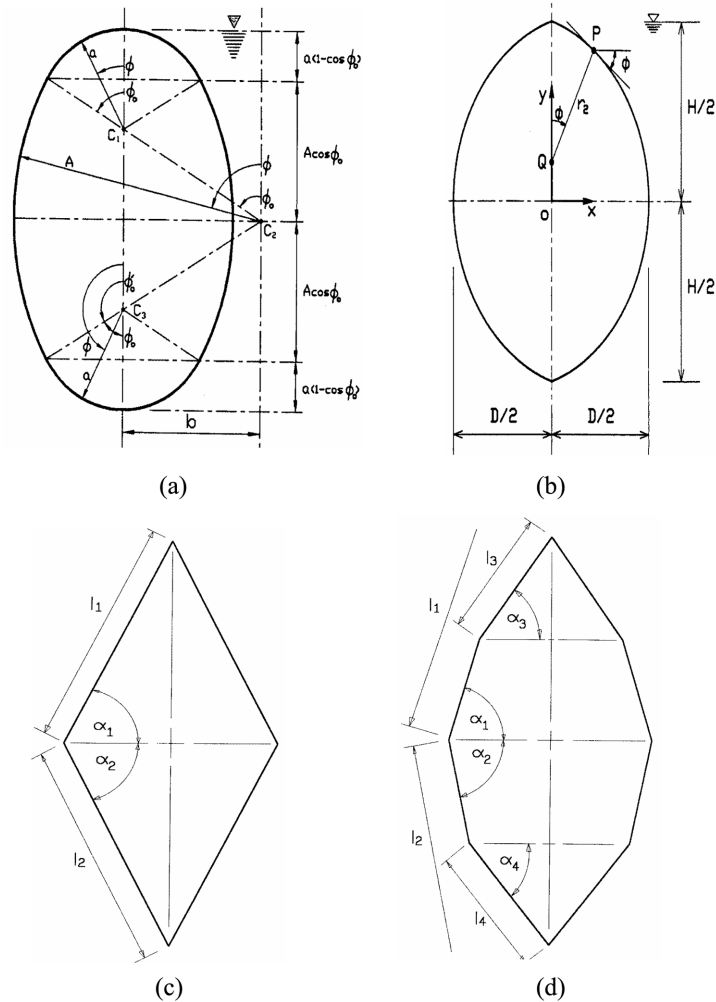


Fig. 2 Some non-conventional forms of sludge digesters: (a) spherical ogival shell with spherical closures, (b) parabolic ogival shell, (c) rhombic shell of revolution, (d) compound cone-frusta assembly

discontinuities over the entire surface of the shell implies a near-membrane state of stress in the entire shell, allowing the study to be conducted solely on the basis of the membrane theory. The stress distribution has been expressed in terms of a single governing parameter, a parametric study undertaken, and some interesting observations noted (Zingoni 2002a).

Given the difficulty and high expense of constructing surfaces/walls of continuously-varying slope (in order to achieve the smoothly-curved “egg” profile), the question arises as to whether or not it would be effective to adopt a series of straight segments for the shell meridian (which are easier and cheaper to construct), while preserving the vertically elongated and good sludge-mixing properties of the basic egg shape. A double-cone or rhombic configuration (Fig. 2c) is the simplest of such an assembly, with the compound cone-frusta variant (Fig. 2d) providing a better solution. The junction stresses of arbitrary cone-cone assemblies have been given in closed form (Zingoni 2002b), and these results can be applied to the sludge-digester configurations in Figs. 2(c) and 2(d).

In this paper, the findings of these separate studies are brought together, some cross-comparisons made, allowing general conclusions to be drawn and design recommendations to be proposed. The closed-form results forming the basis of the theoretical studies have already been validated (Zingoni 2001b, 2002b) via finite-element analyses.

2. The spherical ogival shell

By combining the membrane solution as the particular integral of the general bending-theory equations, and a Geckeler-type edge-zone solution as the homogeneous component, the state of stress throughout the egg shell (Fig. 2a) may be obtained. Details may be seen in the earlier-mentioned papers (Zingoni 2001a,b), in which all analytical results are presented in closed-form, permitting actual stress variations for any given combination of parameters to be readily generated, and any parametric study to be undertaken. Here, we will merely summarise the main observations and conclusions of that study.

Membrane stress resultants N_ϕ^m (force per unit length in the meridional direction) and N_θ^m (force per unit length in the hoop or circumferential direction) in the shell, considered positive when tensile, may easily be determined from equilibrium considerations of a shell element under the applied internal hydrostatic pressure, for each portion of the spherical ogival digester. The results for these, as well as for the deformations V_e^m (meridional rotation) and δ_e^m (lateral displacement) occurring at the edges of each shell region as a result of these membrane actions, are given elsewhere (Zingoni 2001a).

In the vicinity of the junctions of the various shell regions of the digester, the state of stress is mixed, consisting of a membrane component calculated as above, and a bending-related (or edge-effect) component associated with the application of axisymmetric edge bending moments M_e and horizontal shearing forces H_e . A typical junction of the digester is depicted in Fig. 3, in which

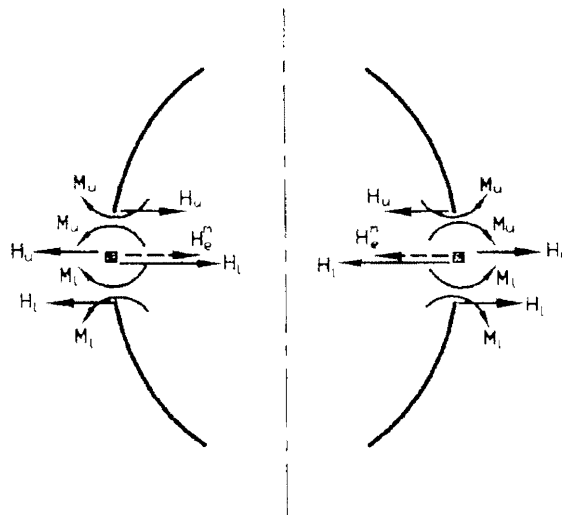


Fig. 3 Generalised junction of the spherical ogival digester, showing actions $\{M_u, H_u\}$ and $\{M_l, H_l\}$ on shell edges and on an inter-edge element of the shell

$\{M_u, H_u\}$ are the actions upon the upper edge of the junction, and $\{M_l, H_l\}$ are the actions upon the lower edge of the junction. By analogy with the flexibility method of structural analysis, these actions are initially regarded as unknown redundants, and are evaluated by imposing the conditions of equilibrium of a shell element lying at the junction of adjacent shell regions (Fig. 3), and the conditions of continuity of deformations V and δ across the junction between two adjacent regions. The results are:

$$M_u = M_l = \frac{\xi K_3 - \mu K_2}{K_4} \quad (1a)$$

$$H_u = H_l = \frac{\mu K_1 - \xi K_2}{K_4} \quad (1b)$$

where

$$\xi = V_l^m - V_u^m \quad (2a)$$

$$\mu = \delta_l^m - \delta_u^m \quad (2b)$$

$$K_1 = I_{11} - J_{11} \quad (3a)$$

$$K_2 = I_{12} - J_{12} \quad (3b)$$

$$K_3 = I_{22} - J_{22} \quad (3c)$$

$$K_4 = (I_{11} - J_{11})(I_{22} - J_{22}) - (I_{12} - J_{12})^2 = K_1 K_3 - K_2^2 \quad (3d)$$

with $\{V_u^m, \delta_u^m\}$ and $\{V_l^m, \delta_l^m\}$ denoting membrane-solution meridional rotations and lateral displacements calculated for the upper and lower edges at the junction (Fig. 3), and the influence coefficients I_{ij} and J_{ij} ($i = 1, 2; j = 1, 2$) being the link between bending-related edge deformations and the bending edge actions for the upper and lower edges at the junction:

$$\begin{bmatrix} V_u^b \\ \delta_u^b \end{bmatrix} = \begin{bmatrix} I_{11} & I_{12} \\ I_{21} & I_{22} \end{bmatrix} \begin{bmatrix} M_u \\ H_u \end{bmatrix} = \begin{bmatrix} -\frac{4\lambda^3}{Etr_1} \left(\frac{r_2}{r_1}\right)^2 & \frac{2\lambda^2}{Et} \left(\frac{r_2}{r_1}\right)^2 \sin \phi_e \\ \frac{2\lambda^2}{Et} \left(\frac{r_2}{r_1}\right)^2 \sin \phi_e & -\frac{2\lambda}{Et} \left(\frac{r_2}{r_1}\right)^2 \sin^2 \phi_e \end{bmatrix} \begin{bmatrix} M_u \\ H_u \end{bmatrix} \quad (4a)$$

$$\begin{bmatrix} V_l^b \\ \delta_l^b \end{bmatrix} = \begin{bmatrix} J_{11} & J_{12} \\ J_{21} & J_{22} \end{bmatrix} \begin{bmatrix} M_l \\ H_l \end{bmatrix} = \begin{bmatrix} \frac{4\lambda^3}{Etr_1} \left(\frac{r_2}{r_1}\right)^2 & \frac{2\lambda^2}{Et} \left(\frac{r_2}{r_1}\right)^2 \sin \phi_e \\ \frac{2\lambda^2}{Et} \left(\frac{r_2}{r_1}\right)^2 \sin \phi_e & \frac{2\lambda}{Et} \left(\frac{r_2}{r_1}\right)^2 \sin^2 \phi_e \end{bmatrix} \begin{bmatrix} M_l \\ H_l \end{bmatrix} \quad (4b)$$

In these matrices, $\{r_1, r_2\}$ are the principal radii of curvature of the shell at the edge, t is the thickness of the shell at the edge, ϕ_e the value of the meridional angle at the shell edge, λ the slenderness parameter of the shell at the edge, and E the Young modulus of the shell material.

The interior actions $\{N_\phi^b, N_\theta^b, M_\phi, M_\theta\}$ (stress resultants and bending moments per unit length, in the meridional and hoop directions) due to the now known edge loads $\{M_u, H_u\}$ (for the upper shell) and $\{M_l, H_l\}$ (for the lower shell) readily follow, and the stresses associated with these bending-related interior actions are superimposed with the membrane stresses to yield the net stresses in the shell:

$$\sigma_\phi^T = \frac{N_\phi^m}{t} + \frac{N_\phi^b}{t} \pm \frac{6M_\phi}{t^2} \quad (5a)$$

$$\sigma_\theta^T = \frac{N_\theta^m}{t} + \frac{N_\theta^b}{t} \pm \frac{6M_\theta}{t^2} \quad (5b)$$

where the upper and lower signs (\pm) associated with the M_ϕ and M_θ terms refer to the inner and outer surfaces of the shell, respectively.

Numerical studies showed that for small to medium-sized egg-shaped digester shells of the spherical-ogival type, junction edge effects are generally not as significant as membrane effects, and the design of the shell will be governed primarily by calculated membrane stresses. The discontinuity effects do alter the *local* meridional stresses significantly, but the net stresses that ensue are considerably lower than membrane stresses elsewhere, so that the stress-raising effect of the discontinuity effects have little bearing on the design of the shell. These conclusions may tentatively be extrapolated to large egg-shaped digester shells of the same basic configuration, but in order to properly investigate the effects of the scale of the structure on the stress levels in the shell, a parametric study should be undertaken.

In order to control the noted steeply increasing membrane meridional compression (which may give rise to buckling problems in the thin shells of the type in question) and membrane hoop tension (which may give rise to cracking problems in the concrete) as one moves downwards from the lower junction of the digester through the lower spherical closure towards the bottom, a number of measures have been recommended. First, the shell thickness t of the lower spherical closure should be increased rapidly with distance s from the shell edge. This thickness enhancement may, for instance, be in accordance with a parabolic law ($t = t_o + ks^2$), which would decrease the stresses almost as rapidly as the membrane stress resultants N_ϕ^m and N_θ^m are rising. Above the lower junction ($\phi = \phi'_o$), and moving upwards, the shell thickness may continue to be decreased within the middle ogival shell in accordance with the law $r_2 t = at_o$ (where r_2 is the distance from the axis of revolution of the digester shell, of a point on the shell midsurface, measured along the normal to the shell midsurface), until $\phi = 90^\circ$ is reached, beyond which the shell thickness may be kept constant at t_o in the upper half of the ogival shell and throughout the upper spherical closure. The reason for prescribing a constant minimum thickness in the upper half of the digester shell is that stress levels in these regions are generally small to moderate.

Alongside the shell thickening recommended in the lower half of the digester shell, tensile reinforcement must be provided, or prestressing adopted, and the levels of these progressively increased as one moves from the equatorial level of the digester towards the bottom.

As the final measure for controlling the steeply increasing membrane stresses in the lower

spherical closure, it has been recommended that the support ring of the digester, or the edge of the shell-ground interactive surface in the case of ground-supported digesters, be raised to 45° from the downward direction of the axis of revolution of the digester shell (that is, $\phi_s = 135^\circ$). This raising of the support level will cut off the very excessive membrane stresses that would otherwise occur towards the bottom of the tank.

3. The parabolic ogival shell

The equation of the generating meridian of the shell of revolution, when the origin of the xy coordinate system is taken at the centre of the digester (Fig. 2b), is

$$y = \pm \frac{H}{\sqrt{2D}} \left(\frac{D}{2} - x \right)^{1/2} \quad (6a)$$

where H is the overall height of the digester and D the equatorial diameter. By reference to Fig. 2(b), the horizontal coordinate x may be expressed in terms of the meridional angle ϕ (equal to the angle between the horizontal and the tangent to the shell meridian at the point in question) as follows:

$$x = \frac{4D^2 \sin^2 \phi - H^2 \cos^2 \phi}{8D \sin^2 \phi} \quad (6b)$$

Owing to the smoothness of the shell geometry and the loading, the membrane solution will suffice over most of the shell, except in the lowermost part that is ground-supported, or adjacent to the circumferential line of vertical supports. For the digester filled to capacity with liquid of weight γ per unit volume, the membrane stress distribution over most of the shell may be expressed in the non-dimensional form (Zingoni 2002a)

$$\begin{aligned} \frac{N_\phi}{\gamma H^2} = & \frac{\xi}{16} \left(\frac{\sin \phi}{4 \sin^2 \phi - \xi^2 \cos^2 \phi} \right) \left[- \left(\frac{4 + \xi^2}{\sin^2 \phi} \right) + \left(\frac{\xi^2}{2 \sin^4 \phi} \right) - \xi(4 + \xi^2) \left(\frac{\cos \phi}{\sin \phi} \right) \right. \\ & + \frac{\xi}{3} (4 + 2\xi^2) \left(\frac{\cos \phi}{\sin^3 \phi} \right) (1 + 2 \sin^2 \phi) - \frac{\xi^3}{15} \left(\frac{\cos \phi}{\sin^5 \phi} \right) (3 + 4 \sin^2 \phi + 8 \sin^4 \phi) \\ & \left. + \frac{1}{30 \xi^2} (112 + 120 \xi^2 + 15 \xi^4) \right] \quad (7a) \end{aligned}$$

$$\begin{aligned} \frac{N_\theta}{\gamma H^2} = & \frac{1}{32 \xi^2} (4 \sin^2 \phi - \xi^2 \cos^2 \phi) \left[\left(\frac{2 \xi \sin \phi - \xi^2 \cos \phi}{\sin^4 \phi} \right) - \left(\frac{\xi \sin \phi}{4 \sin^2 \phi - \xi^2 \cos^2 \phi} \right) \right. \\ & \times \left[- \left(\frac{4 + \xi^2}{\sin^2 \phi} \right) + \left(\frac{\xi^2}{2 \sin^4 \phi} \right) - \xi(4 + \xi^2) \left(\frac{\cos \phi}{\sin \phi} \right) + \frac{\xi}{3} (4 + 2\xi^2) \left(\frac{\cos \phi}{\sin^3 \phi} \right) (1 + 2 \sin^2 \phi) \right. \\ & \left. \left. - \frac{\xi^3}{15} \left(\frac{\cos \phi}{\sin^5 \phi} \right) (3 + 4 \sin^2 \phi + 8 \sin^4 \phi) + \frac{1}{30 \xi^2} (112 + 120 \xi^2 + 15 \xi^4) \right] \right] \quad (7b) \end{aligned}$$

where N_ϕ and N_θ are, of course, the membrane stress resultants in the meridional and the hoop directions respectively, and $\xi = H/D$ (the height-to-diameter ratio of the vessel). (In this section, we have dropped the superscript m for membrane effects, since the meaning is understood.)

The above analytical results show that for tanks with the same shape (that is, tanks of the same height-to-diameter ratio ξ), stress resultants in the shell are directly proportional to H^2 (or to D^2 , since $D \propto H$). For instance, doubling the height H or diameter D of the tank, while maintaining the parameter ξ constant, will quadruple the stress resultants N_ϕ and N_θ in the shell. This is how the *scale* of the structure will affect its design. In Fig. 4, non-dimensional stress resultants have been plotted versus the meridional angle ϕ , for various values of ξ ranging from 1.0 to 3.0, which covers the most practical proportions for egg-shaped sludge digesters.

For all values of the parameter ξ , hoop stress resultants N_θ remain positive (tensile) throughout the parabolic digester, rising from zero at the apex ($\phi = \phi_0$), to some peak value below the equatorial level, before beginning to drop in magnitude with further increase in ϕ . In terms of the non-dimensional stresses $N_\theta/\gamma H^2$, the magnitude and location of this peak value are approximately $\{0.46; 143^\circ\}$, $\{0.24; 129^\circ\}$, $\{0.16; 118^\circ\}$, $\{0.125; 110^\circ\}$ and $\{0.100; 107^\circ\}$ for $\xi = 1.0, 1.5, 2.0, 2.5$ and 3.0, respectively (Fig. 4b). Thus, for a given height H of the digester, the peak value of the hoop stress resultant N_θ increases rapidly as ξ is reduced from 3.0, through 2.5, 2.0 and 1.5, to 1.0 (that is, as the diameter D of the tank is increased). However, the capacity gain as ξ is reduced is more rapid than the increase in the peak hoop stress, implying that structural efficiency increases with reduction in ξ . Here, structural efficiency η is being defined as the ratio of non-dimensional

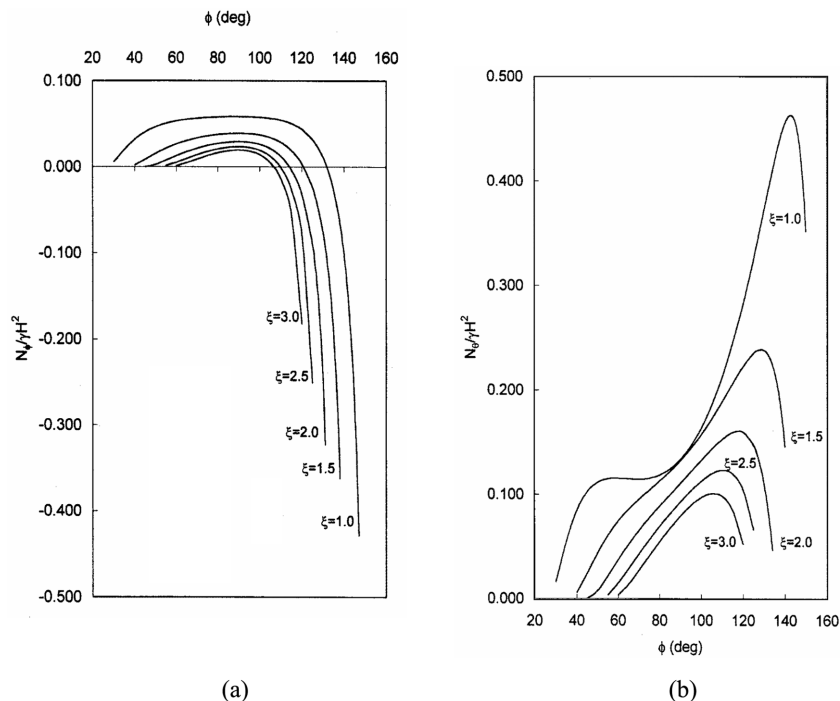


Fig. 4 Non-dimensional stress-resultant variations for the liquid-filled parabolic ogival shell: (a) meridional, (b) hoop

tank volume (volume divided by the cube of the tank height H) to non-dimensional peak hoop-stress resultant. Now the volume of the parabolic ogival vessel may easily be shown to be

$$V = \left(\frac{2\pi\xi}{15}\right)D^3 = \left(\frac{2\pi}{15\xi^2}\right)H^3 \quad (8a)$$

so that the parameter η becomes

$$\eta = \left(\frac{2\pi}{15\xi^2}\right) \left(\frac{(N_\theta)_{peak}}{\gamma H^2}\right) \quad (8b)$$

For $\xi = 1.0, 1.5, 2.0, 2.5$ and 3.0 , the parameter η works out at approximately $0.91, 0.78, 0.65, 0.54$ and 0.47 , respectively.

Turning now to the meridional stress variations (Fig. 4a), it is noted that the stress resultants N_ϕ rise from zero at the apex ($\phi = \phi_o$), to a peak tensile value around the equator ($\phi = 90^\circ$), before beginning to decrease and becoming negative (compressive) in the regions of the tank below the equatorial level. The peak tensile meridional values obtained at the equatorial level are all considerably lower than the peak tensile hoop values that were noted earlier, being approximately (in non-dimensional terms) $0.058, 0.039, 0.029, 0.023$ and 0.019 for $\xi = 1.0, 1.5, 2.0, 2.5$ and 3.0 , respectively.

The crossover from tension to compression occurs at $\phi \approx 132^\circ, 120^\circ, 114^\circ, 110^\circ$ and 106° for $\xi = 1.0, 1.5, 2.0, 2.5$ and 3.0 , respectively. Beyond these changeover values of ϕ , compression rapidly increases with ϕ (that is, with depth of liquid), so that the supports of the tank must be positioned not too far below the changeover values of ϕ in order to cut off the excessive meridional compression that would otherwise occur in the shell were the shell to continue unsupported over its lower regions. This would reduce the likelihood of meridional buckling of the shell in the lower regions. The advantage of locating the supports exactly at the tension-to-compression changeover values of ϕ would be not only the total elimination of zones of compression (and hence of zones of possible local instability), but also the cut-off of the higher hoop-tension peaks (corresponding to $\xi = 1.0, 1.5$ and 2.0).

Assuming, then, that compression in the tank can be eliminated or minimised by careful choice of support location as indicated above, the design of the concrete shell may be based on the hoop and meridional tensile actions. For instance, to cater for the peak hoop tensile non-dimensional stress resultant of 0.46 noted for the case $\xi = 1.0$, one should design the shell to withstand a tensile force of $0.46\gamma H^2$ (per metre width) in the hoop direction. For a very large tank with $H = 50$ m, this force amounts to $0.46(9.81)(2500) = 11\,281.5$ kN/m which, over a shell thickness of say 0.5 m, would result in a tensile stress of 22.6 N/mm² in the material of the shell. Clearly, there would be a need to provide hoop steel reinforcement and/or prestressing to withstand this stress while minimising cracking, and this can easily be achieved following the usual design procedures.

Although the structural efficiency η of the tank as defined herein (that is, ratio of non-dimensional tank capacity to non-dimensional peak hoop-stress resultant) is highest at the lower end of the range of ξ (that is, as ξ approaches 1.0), the range $1.5 \leq \xi \leq 2.0$ is recommended for practical egg-shaped digesters of parabolic ogival profile, since the slope of the shell is sufficiently steep at the poles ($37^\circ \leq \phi_o \leq 45^\circ$) to allow effective prestressing. The overall conclusion of this study is that from a structural and functional point of view, the parabolic ogival profile is suitable for adoption in the design of egg-shaped sludge digester shells.

4. Conical assemblies

It is possible to obtain the state of stress in the conical assemblies of Figs. 2(c) and 2(d) by superimposing the membrane solution due to the hydrostatic internal pressure, with edge effects associated with the junction locations, the latter calculated on the basis of the Geckeler approximation for non-shallow conical shells, or by adopting the one-term asymptotic-series solution for the axisymmetric bending of a non-shallow conical shell (Zingoni 1997, 2002b). Closed-form results for arbitrary cone-cone junction problems have already been derived (Zingoni 2002b), and here we summarise the results for such a junction (Fig. 5).

For the cone-cone shell assembly depicted in Fig. 5(a), where subscripts 1 and 2 denote variables of the upper and lower cones respectively (α being the angle of the cone relative to the horizontal as shown, s the distance coordinate along the sloping meridian measured from the vertex of the cone, and l the value of s at the opening of the cone), edge redundants (that is, axisymmetric shell-edge bending moments and horizontal shearing forces conceptually regarded as the “agents” of the edge effect) $\{M_1, H_1\}$ for the upper cone and $\{M_2, H_2\}$ for the lower cone are shown in Fig. 5(b), while the membrane meridional stress resultants occurring at the shell edges (N_{s1}^m for the upper shell, and N_{s2}^m for the lower shell) are shown in Fig. 5(c).

Horizontal-force and moment equilibrium of an element of the shell at the junction of the two cones (refer to Figs. 5(b) and 5(c)) leads to the relationships

$$H_2 = (N_{s1}^m \cos \alpha_1 + N_{s2}^m \cos \alpha_2) - H_1 \quad (9a)$$

$$M_2 = M_1 \quad (9b)$$

while imposition of the conditions of compatibility of deformations (meridional rotation V and horizontal/lateral displacement δ) between the upper and lower shells at their junction leads to the closed-form solutions

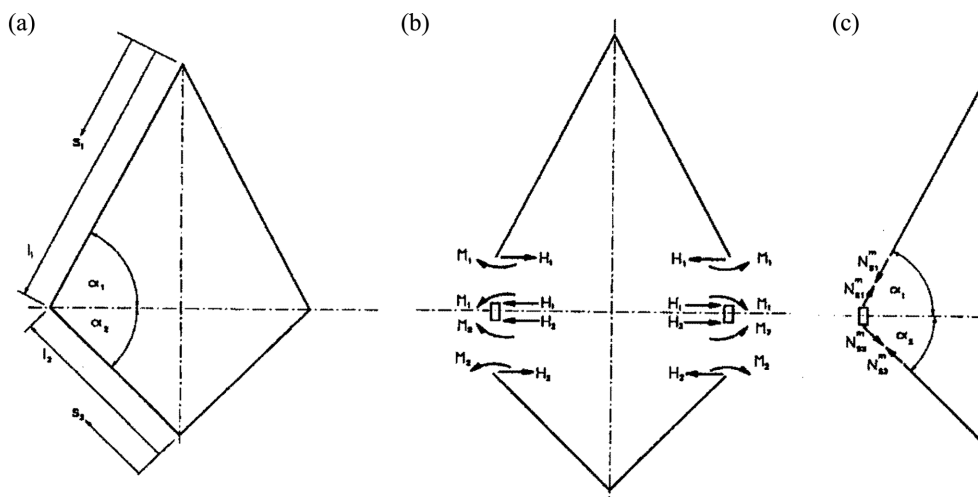


Fig. 5 Arbitrary cone-cone shell assembly: (a) general arrangement, (b) shell-edge bending and shearing actions, (c) shell-edge membrane actions

$$M_1 = \frac{(\sin \alpha_1)(\sin \alpha_2)\{\xi F_a + \sqrt{2}(t_1^2 l_2 \sin \alpha_2 - t_2^2 l_1 \sin \alpha_1)(F_b - F_c)\}}{\eta F_a (\sin \alpha_1)(\sin \alpha_2) + \sqrt{2}(t_1^2 l_2 \sin \alpha_2 - t_2^2 l_1 \sin \alpha_1)(t_2 \omega_1^2 \sin \alpha_2 \cos^2 \alpha_1 - t_1 \omega_2^2 \sin \alpha_1 \cos^2 \alpha_2)}$$

$$H_1 = \frac{\xi(t_2 \omega_1^2 \sin \alpha_2 \cos^2 \alpha_1 - t_1 \omega_2^2 \sin \alpha_1 \cos^2 \alpha_2) - \eta(\sin \alpha_1)(\sin \alpha_2)(F_b - F_c)}{\eta F_a (\sin \alpha_1)(\sin \alpha_2) + \sqrt{2}(t_1^2 l_2 \sin \alpha_2 - t_2^2 l_1 \sin \alpha_1)(t_2 \omega_1^2 \sin \alpha_2 \cos^2 \alpha_1 - t_1 \omega_2^2 \sin \alpha_1 \cos^2 \alpha_2)} \quad (10a, b)$$

where

$$F_a = t_1 l_2 (\cos^2 \alpha_2)(2\sqrt{2}\omega_2 - 4\nu) + t_2 l_1 (\cos^2 \alpha_1)(2\sqrt{2}\omega_1 - 4\nu) \quad (11a)$$

$$F_b = 4Et_1 t_2 (\delta_2^m - \delta_1^m) \quad (11b)$$

$$F_c = t_1 l_2 (\cos^2 \alpha_2)(2\sqrt{2}\omega_2 - 4\nu)(N_{s1}^m \cos \alpha_1 + N_{s2}^m \cos \alpha_2) \quad (11c)$$

$$\xi = \sqrt{2}t_1^2 (l_2 \sin \alpha_2)(N_{s1}^m \cos \alpha_1 + N_{s2}^m \cos \alpha_2) + \frac{Et_1^2 t_2^2}{\sqrt{6(1-\nu^2)}}(V_1^m + V_2^m) \quad (11d)$$

$$\eta = \omega_1 t_2^2 + \omega_2 t_1^2 \quad (11e)$$

The above closed-form results for the shell-edge redundants $\{M_1, H_1, M_2, H_2\}$ are of general applicability. For any given cone-cone assembly under any given applied surface loading, the geometric parameters $\{l_1, \alpha_1, t_1, \omega_1, l_2, \alpha_2, t_2, \omega_2\}$ of the two shells are prescribed quantities, while the membrane stress resultants at the shell edges $\{N_{s1}^m, N_{s2}^m\}$ and the membrane edge deformations $\{V_1^m, \delta_1^m, V_2^m, \delta_2^m\}$ can easily be calculated from the membrane solution, and are therefore assumed to be known. It is important to note that these generalised results for the problem of a conical shell axisymmetrically intersecting another conical shell, such that the vertices of the cones lie on opposite sides of the plane of intersection, are based on the one-term asymptotic-series solution for the axisymmetric bending of a non-shallow conical shell. They are applicable for both complete cones and the larger ends of conical frusta that are not “too short”, provided that $\alpha \geq 30^\circ$ and $l/t \geq 30$, and provided that the shell thickness does not change appreciably in the narrow edge zone of the shell.

With the edge redundants now known, the interior stress resultants $\{N_s^b, N_\theta^b\}$ and interior bending moments $\{M_s, M_\theta\}$ associated with the edge effects then immediately follow (Zingoni 2002b). The final stress distribution for the inner and outer surfaces of the shell are, of course, obtained by superimposing the stresses associated with the edge effects with the stresses associated with the membrane solution:

$$\sigma_s^T = \frac{N_s^b}{t} \pm \frac{6M_s}{t^2} + \frac{N_s^m}{t} \quad (12a)$$

$$\sigma_\theta^T = \frac{N_\theta^b}{t} \pm \frac{6M_\theta}{t^2} + \frac{N_\theta^m}{t} \quad (12b)$$

where σ_s^T refers to the meridional stresses, σ_θ^T refers to the hoop stresses, and t is, of course, the shell thickness.

Preliminary numerical studies have shown that discontinuity stresses around the equatorial junction of the arrangement in Fig. 2(c) are relatively large in comparison with membrane stresses, necessitating the placement of a ring beam there, or the reduction of the slope discontinuity through the adoption of the variant in Fig. 2(d), which has the added benefit of enhancing the containment capacity of the digester for the same overall proportions (height and diameter) of the digester.

5. Comparative study and discussion

As a basis for comparison, let us consider vessels of a similar overall height of 40 m, and a similar equatorial diameter of 20 m, giving a height-to-diameter ratio of 2:1.

In the case of the parabolic ogival shell, these proportions ($H = 40$ m; $D = 20$ m) correspond to a value of 2.0 for the parameter ξ , and give a vessel capacity of $V = 6702$ m³. For this value of ξ , the slope of the vessel at the top and bottom ends of the digester corresponds to $\phi_o = 45^\circ$ which, from a practical point of view, is convenient for prestressing operations.

In the case of the spherical ogival shell of similar overall proportions, choosing a relatively steep junction angle of $\phi_o = 60^\circ$ implies geometric shell parameters of values $a = 6.34$ m, $A = 33.66$ m and $b = 23.66$ m (refer to Fig. 2a), and an overall vessel capacity of $V = 8232$ m³. The more moderate junction angle of $\phi_o = 45^\circ$ implies $a = 2.93$ m, $A = 27.07$ m, $b = 17.07$ m and $V = 7475$ m³.

For a double-cone rhombic configuration of the digester shell, the angle parameters α_1 and α_2 (Fig. 2c) would, of course, be equal, and each 63.4° ($\alpha_1 = \alpha_2 = 63.4^\circ$), giving a vessel capacity of 4189 m³. In terms of capacity, this configuration is relatively inefficient. Modifying it to a compound cone-frusta assembly (Fig. 2d) while preserving the overall height of 40 m and equatorial diameter of 20 m, and while aiming to keep the total angle subtended at the equatorial junction and at the upper and lower off-equatorial junctions *about the same* (i.e., the change in angle at the 3 junctions is the same in moving down the meridian from top to bottom) in order to “balance-out” discontinuity effects, implies that $\alpha_1 = \alpha_2 = 77.5^\circ$ (giving a suitably obtuse subtended angle of 155° at the equatorial junction, from the point of view of minimising junction effects there) and $\alpha_3 = \alpha_4 = 52.1^\circ$ (which is still sufficiently steep, from the point of view of prestressing the shell), with a corresponding enhancement of vessel capacity to $V = 6262$ m³.

Comparing capacities, the spherical ogival digester of $\phi_o = 60^\circ$ is the most efficient container at 8232 m³, followed by its variant of $\phi_o = 45^\circ$ (7475 m³). The parabolic ogival digester comes third at 6702 m³. The conical digesters are the least efficient in terms of retained capacity, at the relatively low capacity of 4189 m³ for the simple rhombic configuration, and the considerably enhanced capacity of 6262 m³ for its cone-frusta variant. Of course, capacities are only one issue here. We also need to assess operational efficiency (the effectiveness of the geometry in facilitating the primary function of a digester with the minimum of maintenance and energy input), costs of initial construction, and structural (load-carrying) efficiency. Intuitively, we know the smoothly curved profiles of the spherical and parabolic ogival shells are more conducive to better mixing of the sludge (and hence are expected to have a higher operational efficiency), but are also more difficult to construct (and hence have higher initial costs), in comparison with conical assemblies. Detailed comparative studies of operational efficiencies and construction costs are beyond the scope of this paper, but we can focus some attention on structural efficiency by examining stress levels in the various configurations.

For the parabolic ogival shell of $\xi = 2.0$, the maximum tensile stresses in the shell are associated

with a non-dimensional hoop stress resultant $N_\theta/\gamma H^2$ of 0.16 (Fig. 4), which for $\gamma = 9810 \text{ N/m}^3$ and $H = 40 \text{ m}$ yields $N_\theta = 2.51 \text{ MN/m}$.

For the spherical ogival digester, there is the complication of discontinuity effects at the junctions of the spherical ends with the middle ogival section. However, and as shown in the earlier study (Zingoni 2001a,b), these effects at the upper junction are small in relation to the level of membrane stresses in the lower regions of the vessel, while the lower junction for the present combination of parameters (ϕ_o, a, A, b) may reasonably be assumed to lie below the level of the supports for the digester, rendering any consideration of discontinuity effects there irrelevant. Similarly, the membrane stresses in the upper spherical closure are generally small in relation to those in the middle ogival shell, while the lower spherical closure may be assumed to be fully supported by the ground, rendering any calculation of membrane stresses over this region largely unnecessary. Thus, we only need to consider the membrane state of stress in the middle ogival shell of the digester. For $\phi_o = 60^\circ$, the relevant domain for ϕ is thus $60^\circ \leq \phi \leq 120^\circ$, while for $\phi_o = 45^\circ$, the relevant domain for ϕ is $45^\circ \leq \phi \leq 135^\circ$.

Fig. 6 shows the variations with respect to ϕ of membrane meridional and hoop stress resultants (N_ϕ and N_θ) for the two spherical-ogival variants (a) $\phi_o = 60^\circ$ and (b) $\phi_o = 45^\circ$. As with all configurations, meridional compression becomes a problem the closer one moves towards the

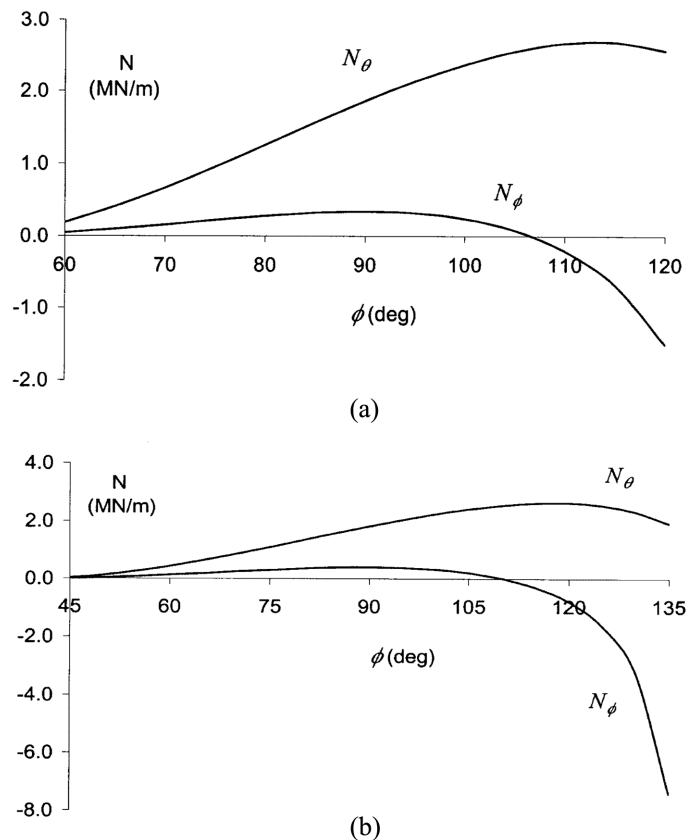


Fig. 6 Variation of membrane stress resultants for the spherical ogival digester (numerical example of comparative study): (a) $\phi_o = 60^\circ$, (b) $\phi_o = 45^\circ$

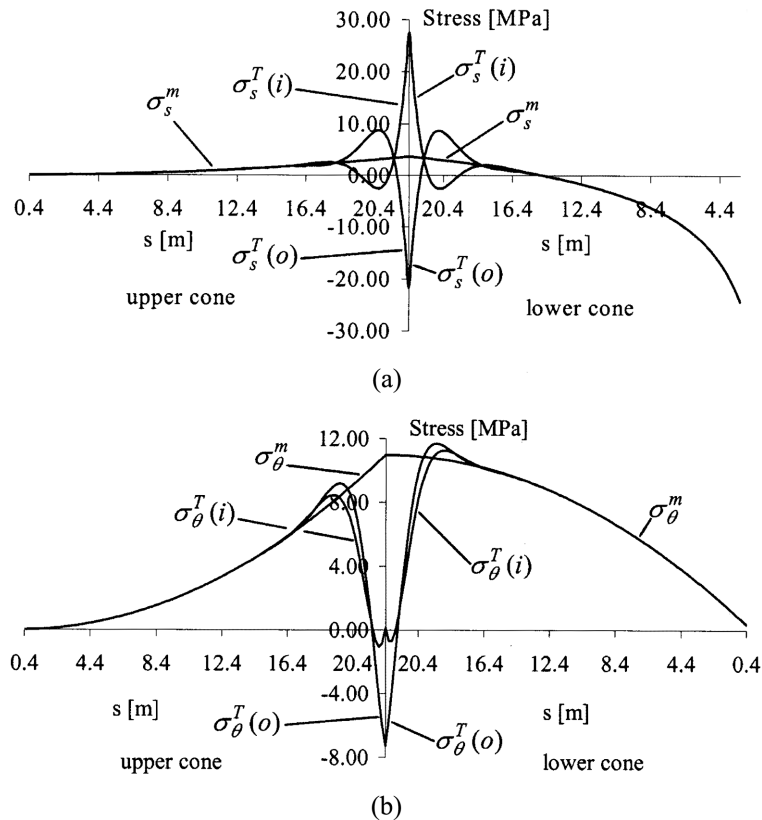


Fig. 7 Variation of stresses around the equatorial junction for the simple double-cone rhombic configuration (numerical example of comparative study): (a) meridional stresses, (b) hoop stresses

bottom of the digester, and this situation can easily be controlled by appropriate shell-thickness enhancement combined with raising of the supports (or rather, upward extension of the supported zone of the digester). It is the concrete-cracking tensile hoop stresses which we want to focus attention on. The stress resultant N_θ peaks at a value of 2.70 MN/m at $\phi = 113^\circ$ for the case $\phi_o = 60^\circ$, and at a value of 2.65 MN/m at $\phi = 118^\circ$ for the case $\phi_o = 45^\circ$. It is interesting to note that these peak values are practically the same, and only slightly bigger than those for the parabolic ogival shell.

For the conical configurations, attention has been focussed on the state of stress around the equatorial junction, which exhibits a high degree of bending. Membrane stresses (σ^m), inner-surface total stresses ($\sigma^T(i)$) and outer-surface total stresses ($\sigma^T(o)$) are shown in Fig. 7 for the simple double-cone (rhombic) configuration and in Fig. 8 for the compound cone-frusta assembly, plotted versus s , the distance from the vertex of the cone (or of the complete cone of which the frustum forms the lowermost part), measured along the sloping meridian. In arriving at these results, a constant shell thickness t of 200 mm has been assumed, with the material parameters E and ν taken as 28 GPa and 0.15 respectively.

In shifting from the configuration of the rhombic digester to the compound cone-frusta digester, the membrane stresses at the equatorial junction reduce rather modestly from 3.5 MPa to 2.5 MPa

(meridional stresses) and from 11.0 MPa to 10.0 MPa (hoop stresses). In terms of stress resultants $N(= \sigma t)$, these reductions are from 0.7 to 0.5 MN/m (meridional) and from 2.2 to 2.0 MN/m (hoop). These last set of figures show that the conical configurations exhibit significantly lower values of hoop tension than the parabolic and the spherical ogival shells of the same height-to-diameter ratio, but the lower value of 2.0 MN/m (corresponding to the compound cone-frusta assembly) is not much lower than the highest value of 2.7 MN/m for the ogival shells.

Comparing the rhombic configuration versus its cone-frusta variant, it is observed that not only is there a considerable gain in containment capacity (from 4189 m³ to 6262 m³) in adopting the latter over the former, but there is also the additional beneficial reduction in junction values of the membrane hoop stress resultant (from 2.2 to 2.0 MN/m), though this hoop stress resultant continues to rise gently to about 2.3 MN/m in moving from the equatorial junction towards the lower edge of the lower conical frustum. (In the simple rhombic configuration, the hoop tension *decreases* in moving down from the equatorial junction through the lower cone.)

Of greater significance is the effect on the discontinuity stresses of altering the conical configuration from simple rhombic to compound cone-frustal. Net meridional stresses at the junction reduce from 27.5 MPa to 11.0 MPa in tension, and from 22.0 MPa to 6.25 MPa in

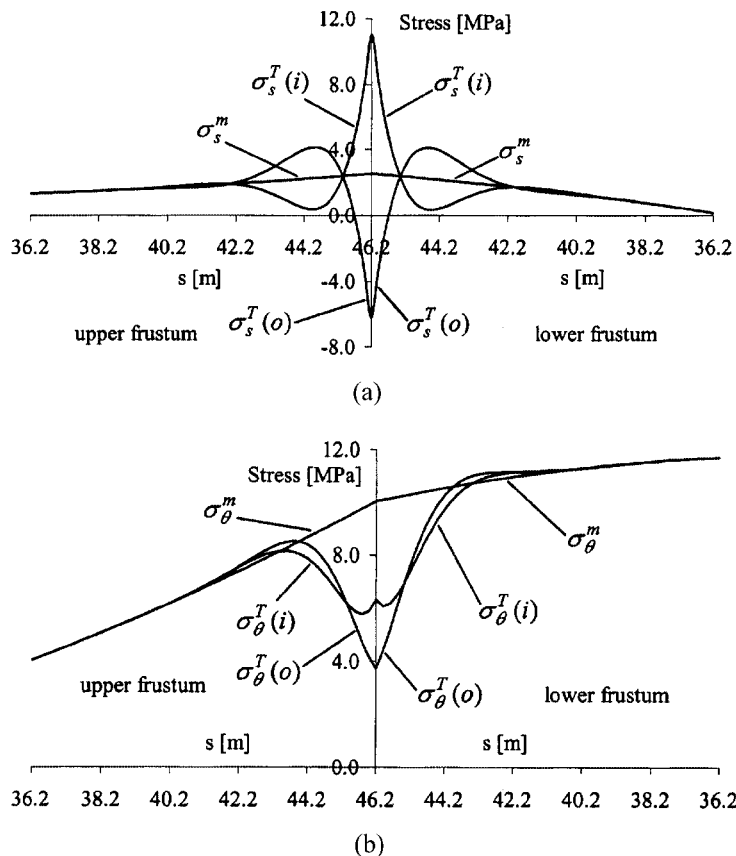


Fig. 8 Variation of stresses around the equatorial junction for the compound cone-frusta configuration (numerical example of comparative study): (a) meridional stresses, (b) hoop stresses

compression, which in terms of “equivalent” stress resultants N (obtained by simply multiplying the total stress by the assumed shell thickness of $t = 0.2$ m, but as the total stress is actually a mixture of direct and flexural stresses, these equivalent stress resultants are not the real stress resultants in the shell), are reductions of 5.5 MN/m to 2.2 MN/m in tension, and 4.4 MN/m to 1.25 MN/m in compression. As is evident by reference to Figs. 7(b) and 8(b), the bending disturbance at the equatorial junction has the effect of inducing hoop compression in the immediate vicinity of the junction, which in the case of the rhombic configuration results in a reversal of the hoop stresses at the junction from tensile (membrane) to compressive (net), but in the case of the compound cone-frusta assembly, the net hoop stresses at the junction still remain tensile but considerably reduced in magnitude.

6. Conclusions

A variety of non-conventional digesters in the form of shells of revolution have been studied, and compared herein with regard to various criteria, particularly structural or load-carrying behaviour. The digester forms investigated have included the spherical ogival shell with spherical end closures, the parabolic ogival shell with pointed top and bottom ends, the rhombic shell (simple double cone) and the compound conical-frustal assembly.

While discontinuity effects are relatively less important at the junctions of the spherical ogival digester, and non-existent in the parabolic ogival digester, they become rather large in comparison with membrane stresses in the case of the conical configurations. Modifying the simple rhombic configuration to a compound cone-frusta assembly not only enhances containment capacity, but also reduces the magnitude of discontinuity stresses quite significantly. The overall conclusion is that the spherical ogival configuration, the parabolic ogival shell and the compound conical-frustal assembly are all feasible forms of digester from the point of view of enhancing proper mixing of the sludge, and efficiently resisting the internal hydrostatic loading, provided that appropriate combinations of shell parameters are chosen, and that the supports are suitably located.

References

- Aeberhard, H.U. (1989), “Egg-shaped digester tanks in Matsumoto City (Japan)”, *IABSE Periodica*, **2**, 32-33.
- Jager, P. (1997), “Two egg-shaped digestors, Australia”, *Struct. Eng. Int.*, **7**(4), 271-274.
- Nojiri, Y. (1989), “Egg-shaped prestressed concrete digester tanks, Yokohama (Japan)”, *IABSE Periodica*, **2**, 30-31.
- Sutter, G. and Jager, P. (1994), “Egg-shaped anaerobic digestors, Taiwan”, *Struct. Eng. Int.*, **4**(3), 160-163.
- Zingoni, A. (2001a), “Stresses and deformations in egg-shaped sludge digesters: Membrane effects”, *Eng. Struct.*, **23**(11), 1365-1372.
- Zingoni, A. (2001b), “Stresses and deformations in egg-shaped sludge digesters: Discontinuity effects”, *Eng. Struct.*, **23**(11), 1373-1382.
- Zingoni, A. (2002a), “Parametric stress distribution in shell-of-revolution sludge digesters of parabolic ogival form”, *Thin-Walled Structures*, **40**(7&8), 691-702.
- Zingoni, A. (2002b), “Discontinuity effects at cone-cone axisymmetric shell junctions”, *Thin-Walled Structures*, **40**(10), 877-891.
- Zingoni, A. (1997), *Shell Structures in Civil and Mechanical Engineering*, Thomas Telford, London.